Bima Journal of Science and Technology, Vol. 8(2B) July, 2024 ISSN: 2536-6041

DOI: 10.56892/bima.v8i2B.739

Improving Textural and Catalytic Properties of Lanthanum-based Perovskite Catalysts for Automotive Exhaust Conversion

Yunus M. M.[1*], Ibrahim I. D.[2] And Shuwa M. S.[3]

[1]Yobe State University, Department of Chemistry, KM. 7, Kashim Ibrahim way Damaturu, ibnyunus2@gmail.com

[2]Yobe State University, Department of Chemistry, KM.7.Kashim Ibrahim Way Damaturu, ibrahimdanyerwa@gmail.com

[3]Ahmadu Bello University, Department of Chemical Engineering, Zaria; (Nigeria).

Corresponding Author: ibnyunus2@gmail.com

ABSTRACT

High cost, limited availability and low thermal stability of noble metals like Platinum, Palladium, Rhodium and Gold used in automotive exhaust emission control has prompted the search for a substitute catalyst with similar activity, better thermal stability and affordability. This work investigated the use of base metals catalysts such as Mn, Co, Ni and Fe to reduce the emission of harmful gases. Perovskites are mixed oxides that have a wide range of properties, such as electrical and magnetic. They are also used as catalysts for eliminating atmospheric pollutants. Silica-supported $LaBO_3$ (B = Mn, Fe, Co, Ni) catalysts were synthesized by deposition-precipitation method, and calcined at high temperature of 800^0C. Properties of the samples were investigated by scanning electron Microscopy-Energy Dispersive X-ray spectroscopy(SEM-EDX), FTIR, X-ray diffraction, Thermogravimetric analysis(TGA) and Brunauer-Emmett-Teller (BET) to survey the morphology and chemical composition, bulk structure, crystalline nature, surface area, thermal stability and porosity of the crystals. The crystallite sizes range between 25--41nm, and specific surface area of 16--219m^2/g. $LaNiO_3/SiO_2$ presented the highest textural values (i.e. smallest crystallite size, highest specific surface area and pore volume) which are beneficial for high catalytic performance. It also exhibits better catalytic activity for oxidation of HC, CO and NO. At 300^0C, the catalyst's conversion efficiency, of the three exhaust gases, reaches more than 70%; which can be considered as a potential replacement for the expensive noble metal catalysts.

Keywords: perovskite, $LaMnO_3/SiO_2$, $LaFeO_3/SiO_2$, $LaCoO_3/SiO_2$, $LaNiO_3/SiO_2$, deposition precipitation

INTRODUCTION

The concern about pollutants released by internal combustion engines has increased significantly. Currently, with a very large number of automobiles and stationary power engines worldwide, vehicle exhaust is one of the main causes of air pollution, especially in urban areas. Unburned hydrocarbons (HCs), carbon monoxide (CO), particulate matter (PM), sulphur oxides (SO_x), nitrogen oxides (NO_x), and soot are the main pollutants in the exhaust (Shrikant et al., 2013). Hydrocarbons and CO occur because the combustion efficiency is not 100%. NOx is formed due to high temperature (>1500^{o}C) of the combustion process causing thermal fixation of nitrogen in the air which makes NOx (Zhang et al., 2010). These pollutants have serious damaging effect on both human and ecology of the environment. They participate in photochemical reactions that cause acid rain and are harmful to human health, as they can damage the respiratory system (Jia et al., 2009). Carbon monoxide (CO) has a dangerous effect on human health as it can strongly coordinate with iron in the haemoglobin forming a compound carboxyhaemoglobin that is many times more stable with oxygen which prevents oxygen from going round the body tissues

DOI: 10.56892/bima.v8i2B.739

(Odesina, 2009). Another dangerous emission is that of unburned or partially burned hydrocarbons (HCs).

Nitrogen and sulphur oxides are also major pollutants responsible for the formation of acid rain, with their well-known damage to the ecosystem and to human health. There is an increasing concern about particulate matter (PM), since it brings about respiratory problems, such as asthma, coughing and difficult or painful breathing. Nearly all pollution is related to the burning of fossil fuels. Gasoline is the primary fuel in the internal combustion engine in most of the countries. Approximately, half of all the HCs, CO and NO emitted are associated primarily to the burning of fossil fuels, particularly those produced by gasoline and diesel engines. Several car manufacturers have investigated different engine operational parameters in order to reduce HCs, CO and NO emissions (Wang et al.,2018). Recently, catalysis technique adopted to oxidize NO to NO_2 has been attracting enormous attention due to its role in several catalytic processes, such as NO_x reduced by selective catalytic reduction (SCR) with hydrocarbons and soot combustion in the atmosphere of NO_x/O_2. Some oxidation catalysts cannot only oxidize HCs, CO and particulate matter (PM), but also facilitate the oxidation of NO to NO_2 which is beneficial for NO_x removal (Teraoka, et al., 2006).

Various catalysts such as base metals (Cu, Fe, Ni etc) and noble metals (Pt, Pd, Rh etc) are used to reduce the level of the harmful gases. The best candidates for these processes are noble metals. But because of their high cost and low thermal stability, it has become imperative to develop an alternative catalyst with similar or even higher oxidation efficiency, thermal stability and more sulphur resistant than noble metal-based catalysts (Deniz et al., 2021). Researchers are investigating many catalysts as alternative to noble metals, and perovskites are commonly used as good substitutes to the precious metals. Perovskites are mixed-metal oxides with a general formula, ABO_3. ''A'' is lanthanum or alkaline earth metal with larger radius and has 12-fold coordination with oxygen atoms. ''B'' is transition metal ion with smaller radius and has a 6-fold coordination with oxygen atoms, and oxygen bonds all the two cations. ''A'' cation is responsible for stabilization of the structure, while ''B'' cation is responsible for the catalytic activity (Huiyuan et al.,2015). Perovskites exhibits high catalytic activity. Literature reported that perovskites containing Ni, Co, Mn or Fe showed excellent catalytic activity toward oxidation of CO, NO and HCs, (Rodriguez et al., 2017).

ABO_3 form of perovskites are versatile (have electrical, magnetic, and catalytic application) due to flexibility of the structure which can accommodate a large number of cations into both the ''A'' and ''B'' positions within the same crystalline structure. Partial or complete substitution of ''A'' and ''B'' sites of perovskite affect its activity. The B site of perovskite is considered to be its catalytic activity site. Therefore, partial or complete substitution of the B with other transition elements can directly influence the catalytic activity of the perovskite (Seyfi et al.,2009). The main drawback of perovskite-based catalyst is its low surface area and also finding good and compatible cation that will result in an excellent physicochemical and catalytic activity. These limitations can be overcome by supporting the perovskite over a high surface area material, like silica (SiO_2) or titania (TiO_2); and to find the ''B'' element that can be compatible with the ''A'' cation. The performance of catalysts is function of their properties. Lanthanum-based perovskites containing transition metal in B-site, ($LaBO_3$, B = Co, Fe, Ni or Mn), show catalytic activity close to the noble metals, presenting low cost and high thermal stability (Szabo et al., 2009). Lanthanum-based perovskites are being studied due to their excellent NO, CO and HCs, oxidation conversion and structural stability (Taguchi

DOI: 10.56892/bima.v8i2B.739

et al., 2002). The catalysts have to be supported on a porous solid material in order to spread the perovskite particles to expose more active sites.

The efficiency of these materials depend on the synthesis method. Many methods are available for the synthesis of perovskite oxide materials such as solid-state reaction, solution combustion synthesis, hydrothermal synthesis, and microwave and reverse micro emulsion process, etc. The main objective to carrying out this study is to comparatively evaluate the physical and chemical properties, as well as the catalytic activity of four simple perovskite catalysts with varying transition elements composition for the conversion of automotive exhaust gases; using a simple, quick and inexpensive method of preparation.

MATERIALS AND METHODS

Preparation of Perovskites

$LaBO_3/SiO_2$ (B = Mn, Fe, Co, Ni) supported perovskites catalysts were synthesized by deposition precipitation (DP) method. The method was adopted from Andrew Justin with slight modification. First, 2.0 g of $La(NO_3)_3.6H_2O$ and $MnCl_2.4H_2O$, each, were dissolved in distilled water to form a solution of the precursor. 6.0 g of the support, SiO_2, was added to the mixture and stirred vigorously. 2M solution of NaOH was slowly added with constant stirring to precipitate the hydroxides of the metals, at room temperature. The precipitate was collected by centrifugation, filtered and washed thoroughly with distilled water repeatedly to get rid of impurities. The precipitate was dried in an oven at temperature of 105^oC for 1hr and 30 min, consequently; the sample was calcined in a muffle furnace at 800^oC for 2hrs to convert the hydroxides to $LaMnO_3/SiO_2$ perovskite. Same procedure was followed for the preparation of $LaFeO_3/SiO_2$, $LaCoO_3/SiO_2$ and $LaNiO_3/SiO_2$ by using $FeCl_3$, $CoCl_2.6H_2O$ and $Ni(NO_3)_2.6H_2O$ precursors, respectively. The final products were ground and kept in muffle furnace and calcined at 800°C for 2 hours (see flow chart Deposition-precipitation synthesis method in Fig: 1.0). The synthesized perovskite samples were characterized by X-ray diffraction (XRD), scanning electron microscopy (SEM), compositional analysis (EDX), Fourier transform infrared (FTIR), Brunauer-Emmett-teller (BET), and Thermogravimetric Analysis (TGA). The catalytic activity, of the catalysts, for oxidation of HC, CO and NO, discharged by gasoline driven engines, was evaluated using a fixed bed reactor and gas analyser.

Physical–Chemical Characterization of the Perovskites

The specific surface area (S_{BET}) of the samples was determined from the nitrogen sorption isotherms at the temperature of liquid nitrogen using the standard Brunauer, Emmet and Teller method (Oluwaiye, 2019). Adsorption/desorption isotherms were obtained using a Micrometrics ASAP 2020M physisorption analyser, after out gassing of samples at 300^oC. The pore size distribution (PSD) was obtained using BJH (Barret–Joygner–Halenda) method.

Information about the crystallinity and crystallite sizes of the samples were obtained by X-ray diffraction (XRD) at room temperature. The XRD analysis were performed on a PANalytical operating at 0kV and 0mA with Cu $K\alpha_1$ radiation source (λ=0.154056nm) at a step time of 1.00s in the bragg angle (2 theta) range 10 to 80. The average crystallite sizes were estimated using the Scherrer equation:

Equation 1: average crystallite sizes of perovskites samples

$$dxRD = k\lambda/\beta\cos(\theta)$$

Where **K** is a constant (0.9)**, λ** is radiation wavelength, **β** is the half width of the peak and **θ** is the Bragg diffraction peak angle.

DOI: 10.56892/bima.v8i2B.739

To get information about the chemical makeup of the samples as determined by vibration of certain functional groups and the nature of chemical bonds present in the materials, FTIR spectroscopy was carried out by grinding the sample with KBr and then scanning it at a wave number 4000–500 cm^{-1}, using the FTIR spectrometer (M530 BUK Scientific Company).

The morphology and chemical components of catalyst were determined using SEM-EDX analysis. Images are obtained at the magnification of 300X. This technique uses a beam of electron that generates signals at the surface of the solid sample. From this, different information such as morphology, composition (chemical) and crystalline structure can be derived. The technique is used to obtain the surface image (with a magnification up to 100.000 times) of a sample and some information about the structural properties of materials. SEM is equipped with an EDX spectrometer for elemental composition analysis.

TGA (Thermogravimetric Analysis) is one of the thermal methods of analysis that is used for measuring the thermal stability of a material. In this method, changes in the mass of a material are measured as the temperature is increased. In order to determine the thermal stability of the synthesized perovskite products, $LaMnO_3/SiO_2$, $LaFeO_3/SiO_2$, $LaCoO_3/SiO_2$ and $LaNiO_3/SiO_2$, Thermogravimetric (TG) has been carried out. The samples were heated at a heating range of 30 to 950°C at 10°C min^{-1} using a Perkin Elmer TGA 4000 simultaneous TG analyzer.

Catalytic Activity Evaluation

The catalytic activity for oxidation of HC, CO and NO discharged by gasoline driven engines was evaluated using reactor and gas analyzer. The catalyst was packed into the reactor supported by iron sponge. The catalyst's activity was measured as a function of temperature at the rate of 5^0C/min. The activity was measured at steady exhaust flow rate of all the four catalysts at same loadings of 0.5 g to study their conversion capacity. The inlet and outlet exhaust concentrations were measured at varying temperature of 300^0C and 400^0C using an NHA-506EN automotive emission analyzer (Nanhua Instruments Co., LTD). The conversion percent of the pollutant gases were calculated using the equation:

Equation 2: Conversion percent of pollutant gases: $X_i = \frac{C_{in} - C_{out}}{C_{in}} * 100\%$

Where C_{in} and C_{out} are the inlet and outlet gas concentration, respectively; and i = HC, CO or NO.

RESULTS AND DISCUSSION

X-rays Diffraction Analysis

Table 1 presents XRD parameters and crystalline sizes identified by XRD measurements for all the four samples of catalysts. This table proves the crystallinity of all samples prepared by deposition precipitation method. The particle sizes were found to be in the range of 29-41nm. The diffraction patterns of all the samples are extremely sharp indicating the existence of highly crystalline materials.

DOI: 10.56892/bima.v8i2B.739

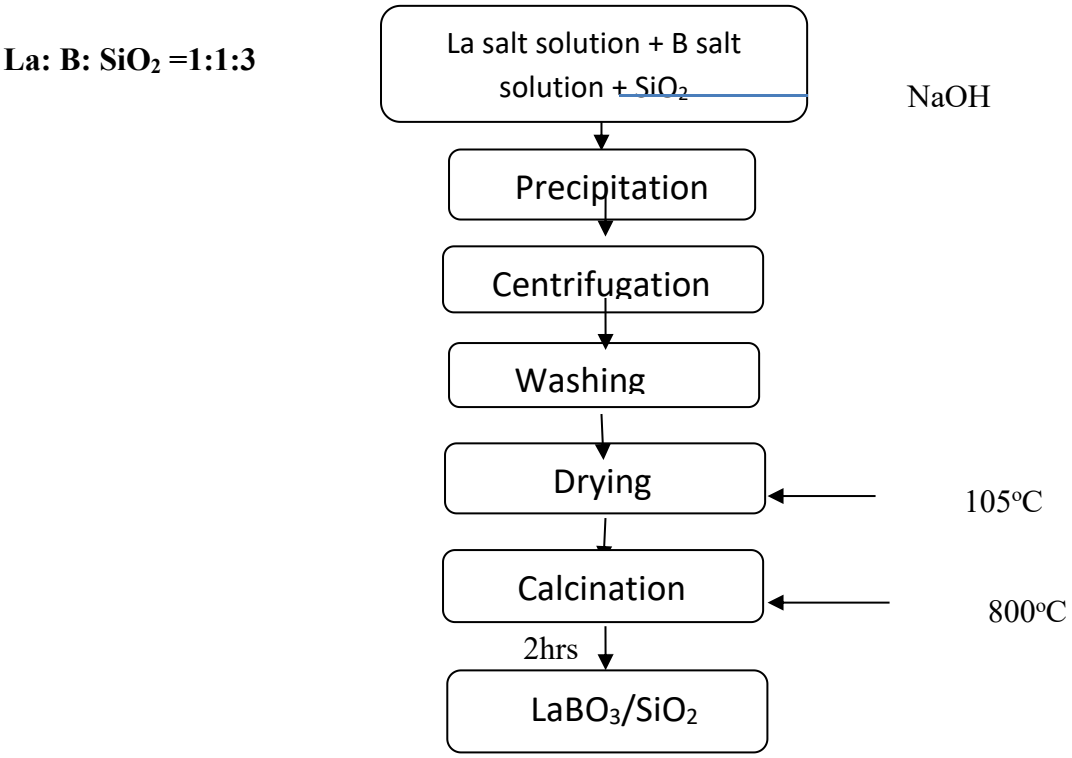

Fig: 1.0 Deposition precipitation synthesis method
(One-pot preparation procedure of $LaBO_3/SiO_2$)

Table 1: Crystallites size of the synthesized catalysts calculated using the Scherrer equation.

Sample	2θ	Intensity %	d-spacing (Å)	β (FWHM)	Crystallite size (nm)
$LaMnO_3/SiO_2$	22.65	100	3.93	0.315	37.97
$LaFeO_3/SiO_2$	21.86	100	4.07	0.280	29.36
$LaCoO_3/SiO_2$	21.79	100	4.08	0.196	41.13
$LaNiO_3/SiO_2$	22.25	100	5.37	0.315	25.71

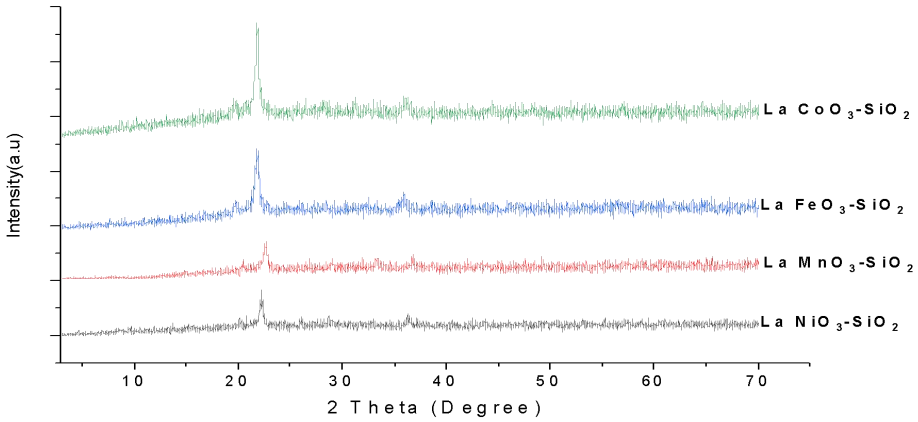

Figure: 2.0 XRD profiles of $LaCoO_3/SiO_2$ (green), $LaFeO_3/SiO_2$ (blue), $LaMnO_3/SiO_2$ (red) and $LaNiO_3/SiO_2$ (black).

Bima Journal of Science and Technology, Vol. 8(2B) July, 2024 ISSN: 2536-6041

DOI: 10.56892/bima.v8i2B.739

Figure 2 depicts X-ray diffraction profiles of the four catalysts as green, blue, red and black for cobalt, iron. manganese and nickel catalysts respectively.

BET Surface Area Analysis and particle size

The specific surface areas of the samples are summarized in Table 2. The specific surface areas of the four catalysts are 15.89m^2/g, 71.07m^2/g, 33.70m^2/g and 219.34m^2/g for $LaMnO_3/SiO_2$, $LaFeO_3/SiO_2$, $LaCoO_3/SiO_2$ and $LaNiO_3/SiO_2$, respectively. The three out of the four prepared catalysts, $LaFeO_3/SiO_2$, $LaCoO_3/SiO_2$ and $LaNiO_3/SiO_2$, in this work, showed higher surface area when compared to the previous work done in some literatures. This is attributed to dispersing the catalysts on high surface area support. $LaNiO_3/SiO_2$ sample showed higher surface area than 188m^2/g $SrTiO_3/SO_2$ synthesized by Oluwaiye (2019).

Sample, $LaNiO_3/SiO_2$, presented the highest specific surface area, 219.34m^2/g with a BJH pore volume of 0.64cm^3g^{-1}. $LaMnO_3/SiO_2$, on the other hand, recorded the lowest specific surface area, 15.89m^2/g and pore volume of 0.063cm^3/g.

Table 2: Brunauer–Emmett–Teller (BET) surface area, pore size and pore volume of the synthesized catalysts.

Samples	S_{BET} (m^2/g)	Pore size (nm)	Pore volume (cm^3/g)
$LaMnO_3/SiO_2$	15.89	2.96	0.063
$LaFeO_3/SiO_2$	71.07	3.00	0.296
$LaCoO_3/SiO_2$	33.70	2.94	0.078
$LaNiO_3/SiO_2$	219.34	2.24	0.644

Elemental Composition and Surface Textural morphology

In order to confirm the formation of $LaMnO_3$, $LaFeO_3$, $LaCoO_3$, $LaNiO_3$ and the presence of SiO_2 composites, EDX analyses were performed. The corresponding peaks are shown in Figure 3, 4, 5 and 6. The elements Mn, Fe, Co, Ni, Si, La and O in the synthesized catalysts can be seen in the EDX spectrums shown in Fig's 3,4,5 & 6. One can see that the samples are not hundred percent pure due to the presence of some foreign elements, carbon, in all the samples. The appearance of the impurities can be attributed to the percentage impurity in the analytical reagents or due to human error. According to the SEM images, the catalysts' surfaces are porous and it appears that the surface particles have agglomerated and cracked, with an irregular shapes and sizes, probably due to high calcination temperature. This can be seen in the images presented in Fig.7.0 (a, b, c & d) for the four synthesized catalysts.

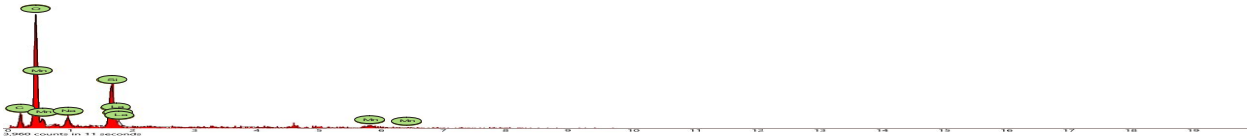

Figure 3: EDX spectrum of $LaMnO_3/SiO_2$

Bima Journal of Science and Technology, Vol. 8(2B) July, 2024 ISSN: 2536-6041

DOI: 10.56892/bima.v8i2B.739

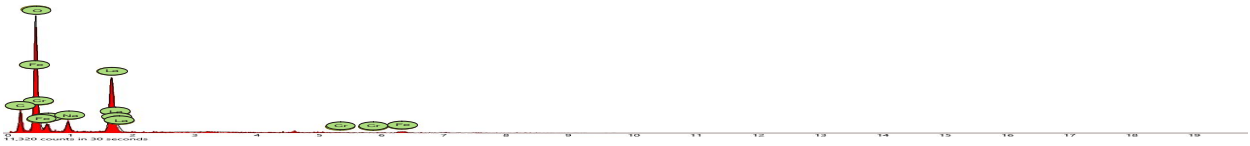

Figure 4: EDX spectrum of $LaFeO_3/SiO_2$

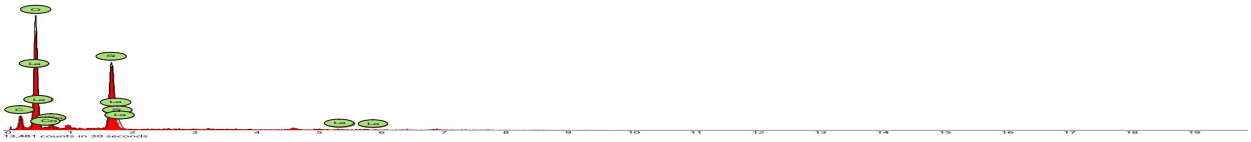

Figure 5: EDX spectrum of $LaCoO_3/SiO_2$

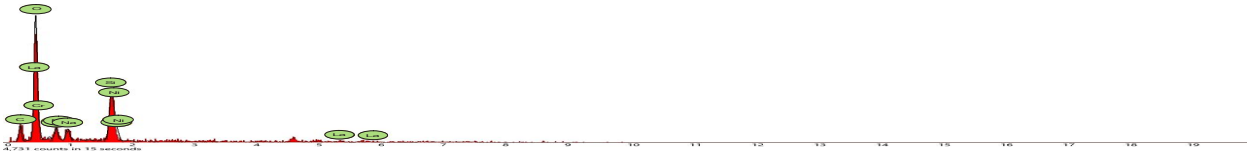

Figure 6: EDX spectrum of $LaNiO_3/SiO_2$

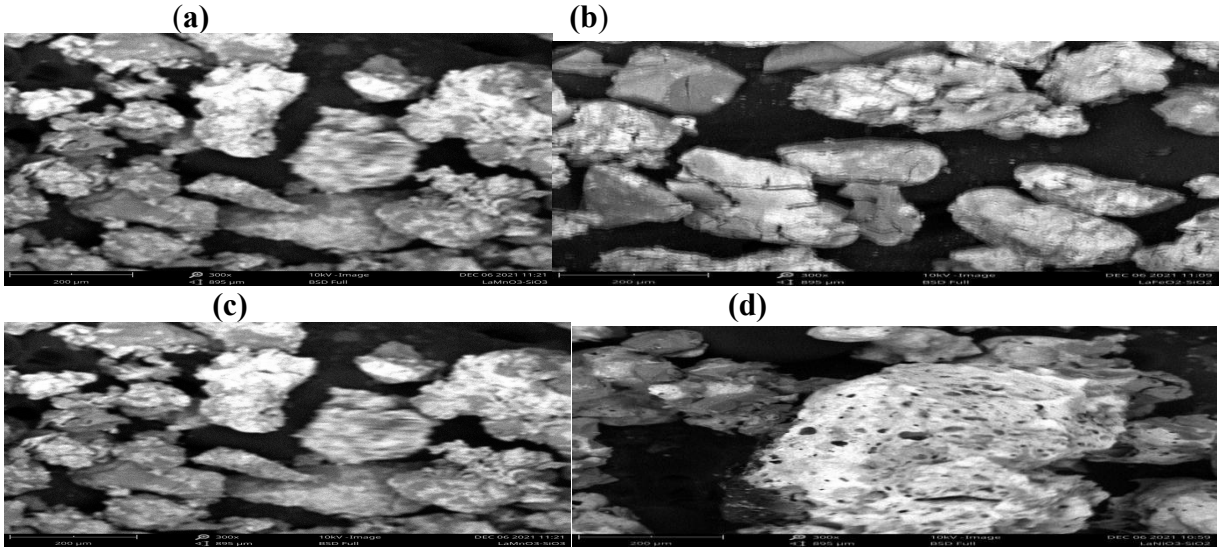

Figure 7: SEM images of the four catalysts:(a) $LaCoO_3/SiO_2$ (b) $LaFeO_3/SiO_2$ (c) $LaMnO_3/SiO_2$ (d) $LaNiO_3/SiO_2$.

FTIR analysis

The multiple FTIR bands in the range of 600-900 cm^{-1} are allotted for different stretching modes of M-O bond on the metal oxide framework (Shafath et al., 2023). As shown in Figure 8, the strong IR band at 1113cm^{-1} is usually assigned to the Si-O-Si asymmetric vibrations. The picks at 668 cm^{-1} and 592 cm^{-1}, corresponding to $LaBO_3$ perovskite coated on SiO_2, are clearly observed in these spectra (Tavakkoli & Moayedipour 2014). The IR vibration bands around 600cm^{-1} could be attributed to the characteristic absorption bands of the stretching vibration of Mn-O, Fe-O, Co-O and Ni-O bands of BO_6 octahedron (Nyamdavaa et al., 2017). The broad band in the region of 3400cm^{-1} and 1640 cm^{-1} is due to the H-O stretching and H-O-H bending

DOI: 10.56892/bima.v8i2B.739

vibration of H_2O molecules adsorbed at the surface of the catalyst, respectively, or the molecule of water of crystallization present in KBr. The strong peak at about 630cm^{-1} arises from the stretching vibration of the Mn-O bond (Chen & He 2009) as shown in Fig. 8.0. The broad absorption band in the region of 600–700 cm^{-1} is assigned to Ni–O stretching vibration mode; the broadness of the absorption band indicates that the NiO powders are nanocrystals (Hongxia et al., 2009). Finally, the band at 610 cm^{-1} is assigned to the vibrations of La-O bond (Deniz et al., 2012).

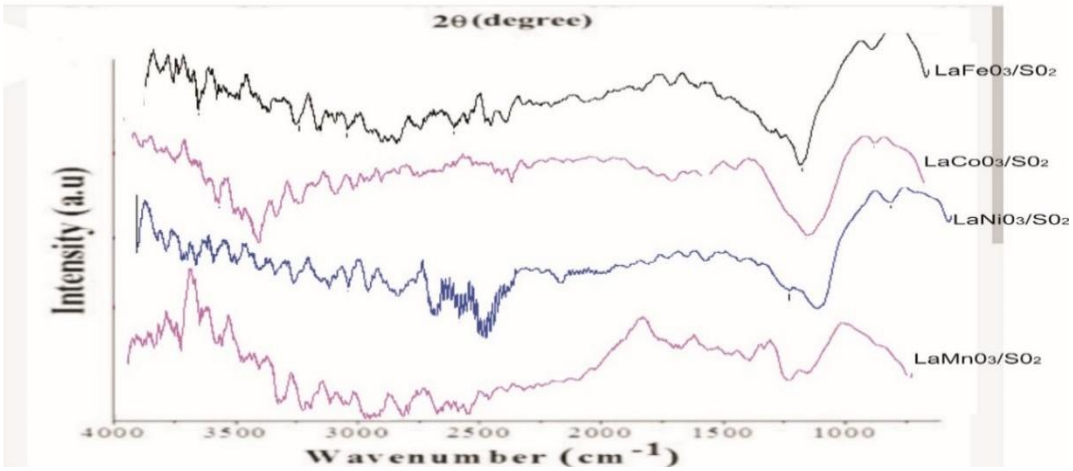

Figure 8: FTIR spectrum of $LaFeO_3/SiO_2$, $LaCoO_3/SiO_2$, $LaNiO_3/SiO_2$ and $LaMnO_3/SiO_2$ particles.

Thermogravimetric Analysis (TGA)

The TGA results of the four samples demonstrate a similar thermal decomposition. This effect could be attributed to the fact that the catalysts are deposited over the same support (SiO_2). The four TGA curves shown in figure 3.5 indicate two weight loss steps in the thermogram profile. The partial one is in the temperature range of 80-180^{o}C, which is about 6% weight loss (Benaicha & Omari 2018), corresponds to dehydration (loss of water). The final, and the massive weight loss, about 83%, between 300 and 510^{o}C, is attributed to decomposition of the samples. At temperature above 510^{o}C, no weight loss is observed indicating their thermal stability at that temperature; more stable than the decomposition temperature of the perovskite samples reported by Yao et al., 2011 (Yao et al., 2011); who synthesized $LaNiO_3$ which decomposed at 155^{0}C. Deniz et al., 2021; used sol-gel method to synthesize $LaMnO_3$ which decomposed at 200^{0}C. The final decomposition product observed at around 513°C is assumed to be the crystalline phase formation of the perovskite catalyst (Akinlolu et al., 2019).

Bima Journal of Science and Technology, Vol. 8(2B) July, 2024 ISSN: 2536-6041

DOI: 10.56892/bima.v8i2B.739

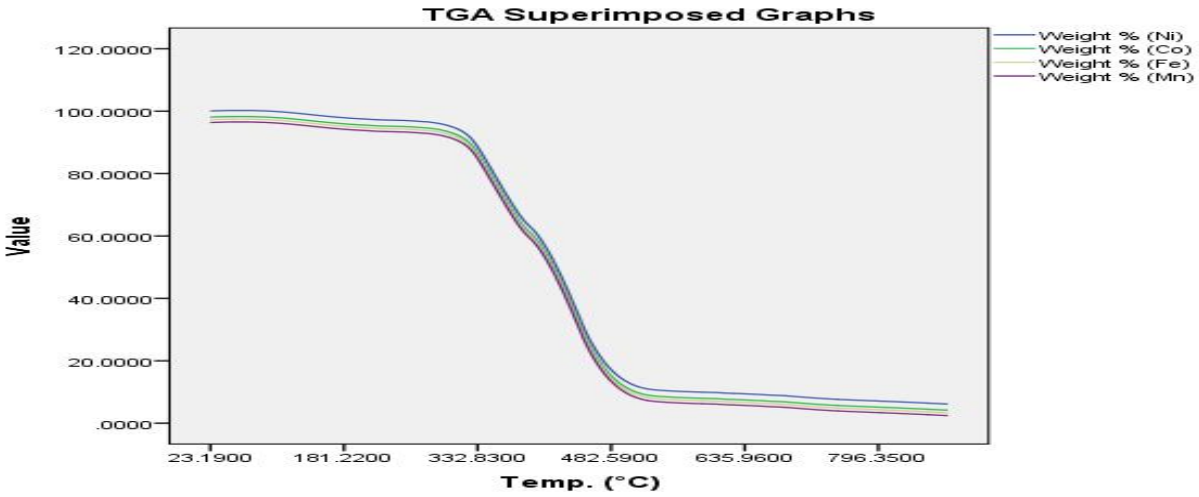

Figure 9: TGA curve showing the thermal decomposition of $LaBO_3/SiO_2$ (B=Mn, Fe, Co, Ni)

Catalytic Activity

Percentage Conversion of Various Catalysts

Table 3: Conversion of emissions at various temperatures

Catalyst	Temperature (^{0}C)	Conversion in % of exhaust gases		
		HC	CO	NO
$LaMnO_3/SiO_2$	300	40.62	67.89	57.29
	400	19.31	46.42	25.00
$LaFeO_3/SiO_2$	300	39.58	58.98	56.25
	400	26.13	45.76	43.18
$LaCoO_3/SiO_2$	300	54.16	60.25	61.45
	400	38.63	52.91	53.41
$LaNiO_3/SiO_2$	300	73.95	77.24	78.12
	400	48.86	56.87	64.77

Table 3.0 represents the catalytic conversion efficiency of the prepared catalysts for the exhaust gases (HC, CO, NO) emitted by gasoline driven generators at varying temperatures of 300^{0}C and 400^{0}C. All the four catalysts showed higher conversion efficiency of all the three gases at lower temperature of 300^{0}C. This shows that catalytic activity of perovskite catalyst is influenced by the reaction temperature. The comparison shown indicates that among the four prepared perovskite samples, $LaNiO_3/SiO_2$ presents the best performance (Table 3.0), with a maximum HC, CO and NO conversion of about 74%, 77% and 78%, respectively, at 300^{0}C. In contrast, $LaFeO_3/SiO_2$ exhibits the lowest activity with 39%, 58% and 56% of HC, CO and NO conversion, respectively. $LaMnO_3/SiO_2$ and $LaCoO_3/SiO_2$ exhibited a fairly good catalytic activity toward converting CO to about 68% and 60% respectively. The conversion efficiency of $LaNiO_3/SiO_2$ catalyst is greater than the conversion efficiency of 25wt% $SrTiO_3/SiO_2$ but lower than 50wt% $SrTiO_3/SiO_2$ synthesized and reported by Oluwaiye, 2019. This demonstrates that loading percentage influences conversion factor.

CONCLUSION

$LaBO_3$ (B = Mn, Fe, Co, Ni) perovskite samples were synthesized using deposition precipitation method. SEM-EDX, FTIR, XRD, TGA and BET techniques showed significant differences in physical properties

DOI: 10.56892/bima.v8i2B.739

of the samples. The low surface area of perovskite catalyst is being enhanced by depositing it over a high surface area support, thereby, increasing the contact between the catalyst and substrates, which can speed up the rate of reaction. Among the four (4) catalysts, $LaNiO_3/SiO_2$ presented the smallest crystallite size, highest specific surface area and pore volume. It also exhibits better catalytic activity for oxidation of HC, CO and NO. At 300^0C, the catalyst's conversion efficiency, of all the three exhaust gases, reaches more than 70%; which can be considered as a potential replacement for noble metal catalysts.

REFERENCES

Akinlolu K., Bangboye O., Ogunniran K., and Tripathi S. (2019). Synthesis and characterization of A site doped lanthanum based perovskite catalyst for the oxidation of soot. IOP, Cof. Series; Materials Science and Engineering 509 01206 IOP Publishing doi:10.1088/1757-899X/509/1/01206

Benaicha A. and Omari M. (2018). Synthesis and Characterization of Perovskite Oxides $LaFe_{1-x}CuXO_3$ ($0 \leq X \leq 0.4$) Obtained By Sol-Gel Method. Journal of Fundamental and Applied Sciences. doi:http://dx.doi.org/10.4314/jfas.v10i1.

Chen H., He J. (2009). Facile synthesis of monodisperse manganese oxide nanostructures and their application in water Treatment. J Phys Chem C, 112:17540–17545

Deniz Ö., Ahmet T., Erdal C. (2021). Synthesis and Characterizations ofLaMnO3Perovskite Powders Using SolGelMethod. Research Square.DOI: https://doi.org/10.21203/rs.3.rs-217058/v1.

Hongxia Q., Zhiqiang W. Hua Y. Lin Z., Xiaoyan Y.(2009). Preparation and Characterization of NiO Nanoparticles by Anodic Arc Plasma Method.. Hindawi Publishing. Corporation Journal of Nanomaterials. Article ID 795928, 5 pages doi:10.1155/2009/795928

Huiyuan Z., Pengfei Z., and Sheng D., (2015). Recent Advances of Lanthanum-Based Perovskite Oxides for Catalysis. ACSCatal. 5,6370−6385. DOI:10.1021/acscatal.5b01667.

Jia L., Gao J., Fang W., Li Q. (2009). Carbon Dioxide Hydrogenation to Methanol over the Pre-reduced$LaCr_{0.5}Cu0.5O_3$ catalyst Commun. DOI:10:20002003.10.1016/j.catcom.2009.07.017

Nyamdavaa E., Uyanga E., Sevjidsuren G., and Altantsog P., (2017). Lanthanum-Based Perovskite-Type Oxides $La_{1-x}CexBO_3$ (B= Mn and Co) as Catalysts: Synthesis and Characterization.

Odesina, I. A. (2009). Essential Chemistry.TONAD. Ibafo, Ogun state.

Oluwaiye, U. E. (2019). Synthesis of $SrTiO_3/SiO_2$ Perovskite Catalys For the Control of NoxiousEmission from Stroke Engines. (To be published).

Rodriguez D .S., Wada H., Yamaguchi S., Farjas J. (2017). Synthesis of$LaFeO_3$ perovskite-type oxide via solid-state combustion of a cyano complex precursor: The effect of oxygen diffusion. Ceramics International. 43: 3156-3165.

Seyfi B., Baghalha M., Kazeman H. (2009). Modified $LaCoO_3$ Nano-perovskite Catalysts for the Environmental Application of Automotive CO oxidation. Chem Eng J;143:306–11.

Shafath S. Khulood L. Anchu A. Anand K. Ibrahim M. Reesh A. (2023). Highly Active Lanthanum Perovskite Electrocatalyst (LaMnxCo1-xO3 ($0 \leq x \leq 1$)) by Tuning the Mn:Co Ratio for ORR and MOR in Alkaline Medium Spriger Electrocatalysis.

Shrikant N., Dipti D., Anjali A. (2013). Comparative Study of Lanthanum Based Perovskites Synthesized by

DOI: 10.56892/bima.v8i2B.739

Different Methods Springer-Verlag Berlin Heidelberg. DOI: 10.1007/978 3-64234216, 5_3.

Szabo V., Bassir M. Gallot J. Van Neste A. Kaliaguine S. (2009). Catalytic Oxidation of NO. Appl. Catal. B 42 265.

Taguchi H., Yamada S., Nagao M., Ichikawa Y., Tabata K. (2002). Surface characterization of $LaCoO_3$synthesized using citric acid. Mater Res Bull; 37:69-76. DOI:1016/soo25 5408(01)00799-1.

Tavakkoli H.; Moayedipour T. (2014). Fabrication of perovskite type oxide $La_{0.5}Pb_{0.5}MnO_3$ nanoparticlesand its dye removal performance. J. Nanostruct. Chem., 4, 116 124.

Teraoka Y., Nakano K., Shangguan W. F., Kagawa S. (2006). Simultaneous catalytic removal of nitrogen oxide and diesel soot particulate over perovskite-related oxides. Catal. Today. 27:107–111

Wang H.; Cao Y.; Chen Z.; Yu Q.; Wu S. (2018). High-efficiency removalof NOx over natural mordenite using an enhanced plasma catalytic process at ambient temperature. Fuel, 224, 323 330.

Yao W., Guofang Z., Chengshan L., Guo Y., Yafeng L. (2011). Preparation and Characterization of $LaNiO_3$ films grown by metal–organic deposition. Bull. Mater. Sci., Vol. 34, No. 7, December 2011, pp. 1379–1383. © Indian Academy of Sciences.

Zhang Y., Zhang H., Dai J., Deng L., Wei H. (2010). Catalysis Today.153 (3), 143-149.